INTERNATIONAL ATOMIC ENERGY AGENCY
UNITED NATIONS EDUCATIONAL, SCIENTIFIC AND CULTURAL ORGANIZATION

INTERNATIONAL CENTRE FOR THEORETICAL PHYSICS
34100 TRIESTE (ITALY) - P.O.B. 586 - MIRAMARE - STRADA COSTIERA 11 - TELEPHONE: 2240-1
CABLE: CENTRATOM - TELEX 460392 - I

SMR/384 - 14

EXPERIMENTAL WORKSHOP ON
"HIGH TEMPERATURE SUPERCONDUCTORS"
(30 March - 14 April 1989)

THERMODYNAMICS
Magnetic Behaviour

Francisco DE LA CRUZ
Centro Atomico Bariloche
(8400) San Carlos de Bariloche
Argentina

La Sr Cu O — Ceramic

Y Ba Cu O — " — Single X-tals

Bi Sr Ca Cu O — " — " "

Macroscopic Properties

Normal — Superconducting

Resistivity

Specific Heat

Magnetization : dc - ac

Guimpel
Civale
Osguiguil
Safar
Decca
Pastoriza
Nieva
Martinez

Esparza
D'Ovidio
Fainstein
Petunchi
Schneemeyer
Waszczak
Kapler

THERMODYNAMICS

Ceramics vs. Single Crystals
Why?

Nothing like this happens in traditional metals where
Supercondac. in X-tals = PoliX-tals

In High Tc the sup. in X-tals and ceramics might be ≃ granular sup. in traditional sup.

Why?

Magnetic Glass — Vortices
Reversibility Line — Giant Flux Flow
Trapped Flux — Vortex Pinning

Vortex Melting
Reversibility

Superconduting Lengths

Pair size

Pippard's Argument

Normal properties ~ Free electrons

$$\epsilon = \frac{P^2}{2m^*}$$

Superconducting Properties. Electronic phase transition.

$$\Delta P \Delta x = \hbar \qquad \Delta x \simeq \xi_0$$

$$\Delta P = \frac{\Delta\epsilon\, m^*}{P} \qquad \Delta\epsilon \simeq kT_c$$

$$\xi_0 \approx \frac{\hbar v_F}{kT_c}$$

$$\boxed{BCS \rightarrow \xi_0 \approx 0.2\frac{\hbar v_F}{kT_c}}$$

Interaction ≃ kT_c

Coherence length $\xi_0(\infty) \simeq \frac{\hbar v_F}{kT_c}$

Free Electron

Experimental $\left.\begin{matrix} T_c \\ n \end{matrix}\right\} v_F$

		Free electron	Experiment
LaSrCuO T_c 40K	ξ_p	20 Å	15Å – 40Å
YBaCuO T_c 100K	ξ_p	10 Å	7Å – 40Å
Al T_c 1K	ξ_p	20.000 Å	10.000 Å

Pair density $n_p \approx n \cdot \frac{T_c}{T_F}$

distance between pairs d_p

	d_p	ξ_p / d_p
La Sr CuO	30 Å	~ 1
Y Ba CuO	20 Å	~ 1
Al	100 Å	~ 100

if $\xi_0 \gg d_p$

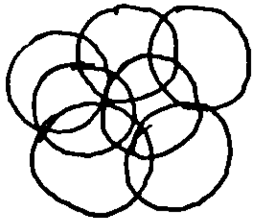

- Complicated fermion system
- BCS mean field } theories $\Psi^2 \simeq n_s$
- Gingborg-Landau }

Effective impurities change T_c only if $\ell \simeq d_p$

ℓ = mean distance between effective impurities

$T_c \neq f(x)$

if $\xi_0 \ll d_p$

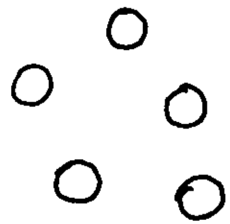

- More complicated
- localized pairs

no m.f. theories

Effective impurities change T_c locally $T_c = f(x)$

High T_c $\xi_0 \simeq d_p$?

$\Longrightarrow$ Theoretical Problems
Experimental Problems

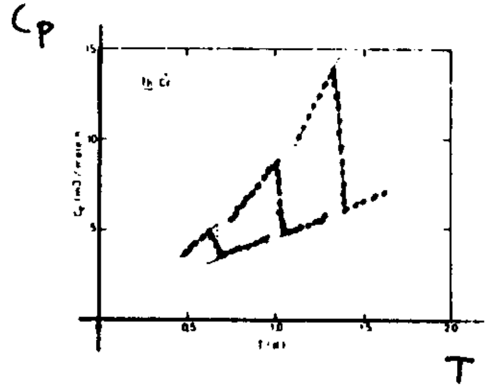

ThCr

Sereni et al
Physica 1981

Example of impurity effects (magnetic) in traditional superconductors

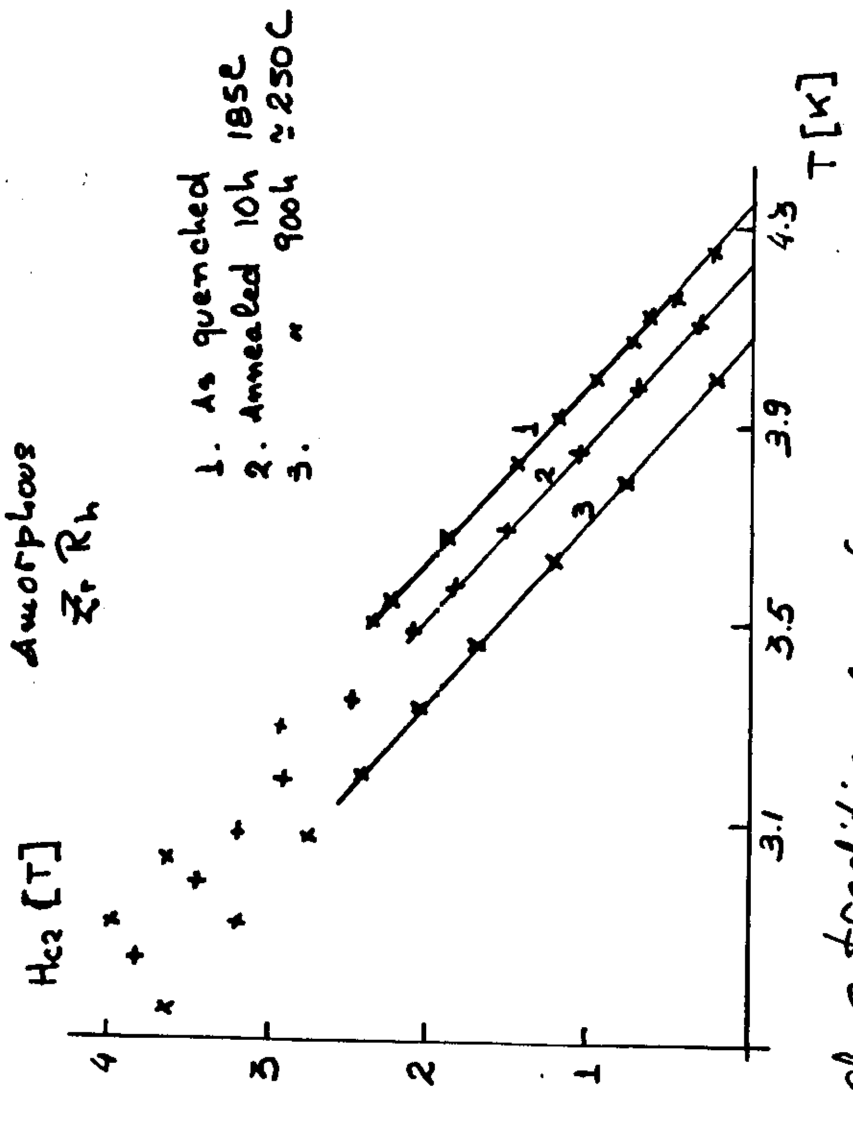

Behavior of a traditional superconductor

(Barilooke's group)

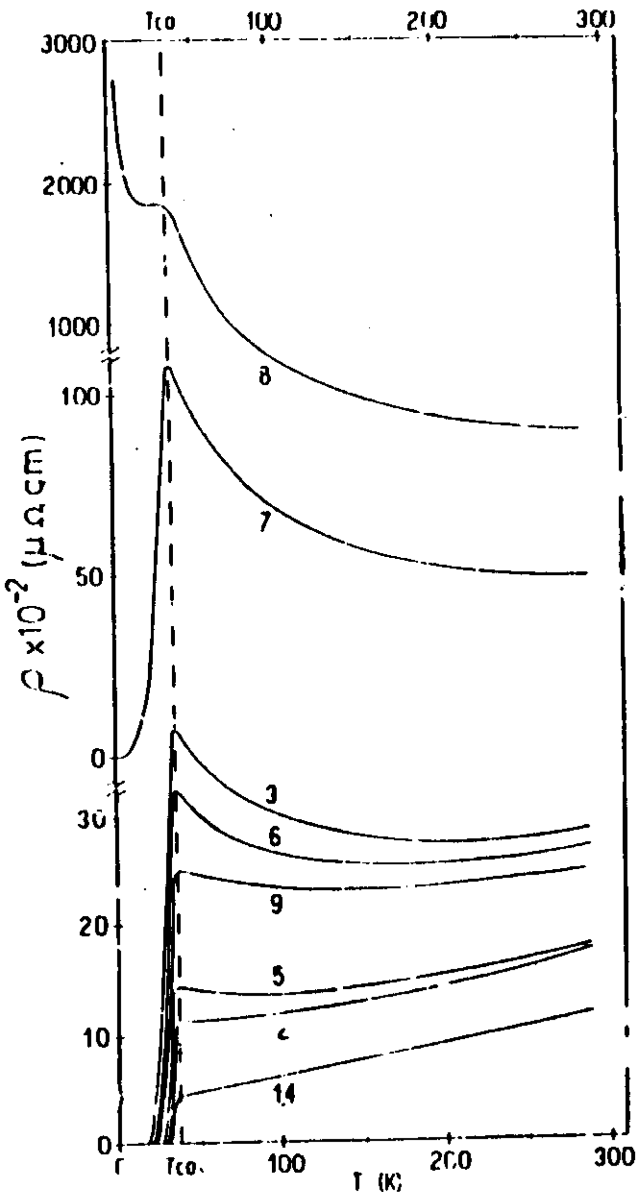

Resistivity and transition temperature
Deoxygenation effects in $La_{1.8}Sr_{.2}CuO_{4-\delta}$

Macroscopic Theories

Ginzburg - Landau

There are 2 distances

$\xi(T) \Rightarrow \Psi(x)$ $\quad \Psi^2(x) = n(x)$

The coherence length determines the cost of energy due to space modulation of the order parameter

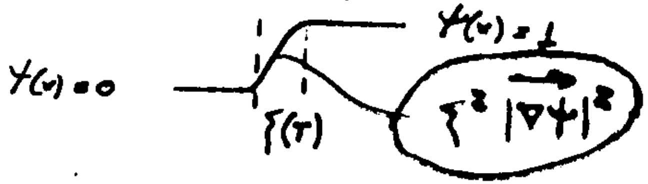

BCS $\quad \xi(0) = .75\,\xi_0 \Rightarrow$ Gorkov

(2) $\quad \lambda(T) \Rightarrow h(x)$

The penetration depth determines the field response

$$\lambda^2 = \frac{m}{\Psi^2 e^{*2}}$$

Origin of the Modulation of the order parameter

Intrinsic	Extrinsic
Vortices	Defects
$H_{c1} - H_{c2}$	point defects?
	extended defects
Atomic structure	chemical
High Tc ?	stechiometry
Boundaries	

In high Tc $\lambda \gg \xi \Rightarrow$ London Model for vortices. Ψ = constant

$$\epsilon_1 = \int_S \left(\frac{1}{2} \frac{m^*}{\Psi^2 e^{*2}} J_s^2 + \frac{h^2}{8\pi} \right) dS$$

$$\epsilon_1 = \frac{\Phi_0^2}{4\pi \lambda^2} \ln K \; ; \quad K = \frac{\lambda}{\xi} \gg 1$$

$$H_{c1} = \frac{\Phi_0}{4\pi \lambda^2_{(T)}} \ln K \; ; \quad \boxed{\lambda^2 = \frac{m^*}{\Psi^2 e^2}}$$

$$H_{c2} = \frac{\Phi_0}{2\pi \xi^2_{(T)}}$$

$H_{c1} \Rightarrow$

H_{c2}

Modulation distances

If $\Psi(x) \Rightarrow 0$ in ξ^2 due to diluted defects the critical fields are not modified.

There is pinning energy at the core $\frac{H_c^2}{8\pi} \times \xi^2$

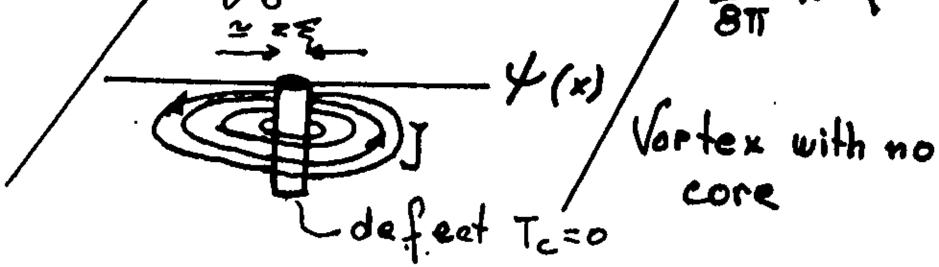

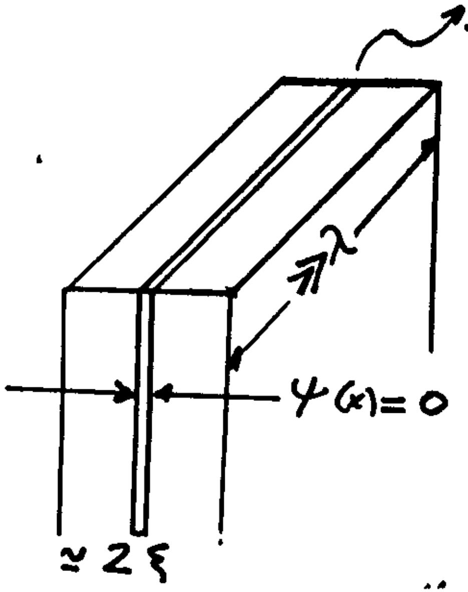

H_{c1} is reduced depends on the size and characteristic of the defect.

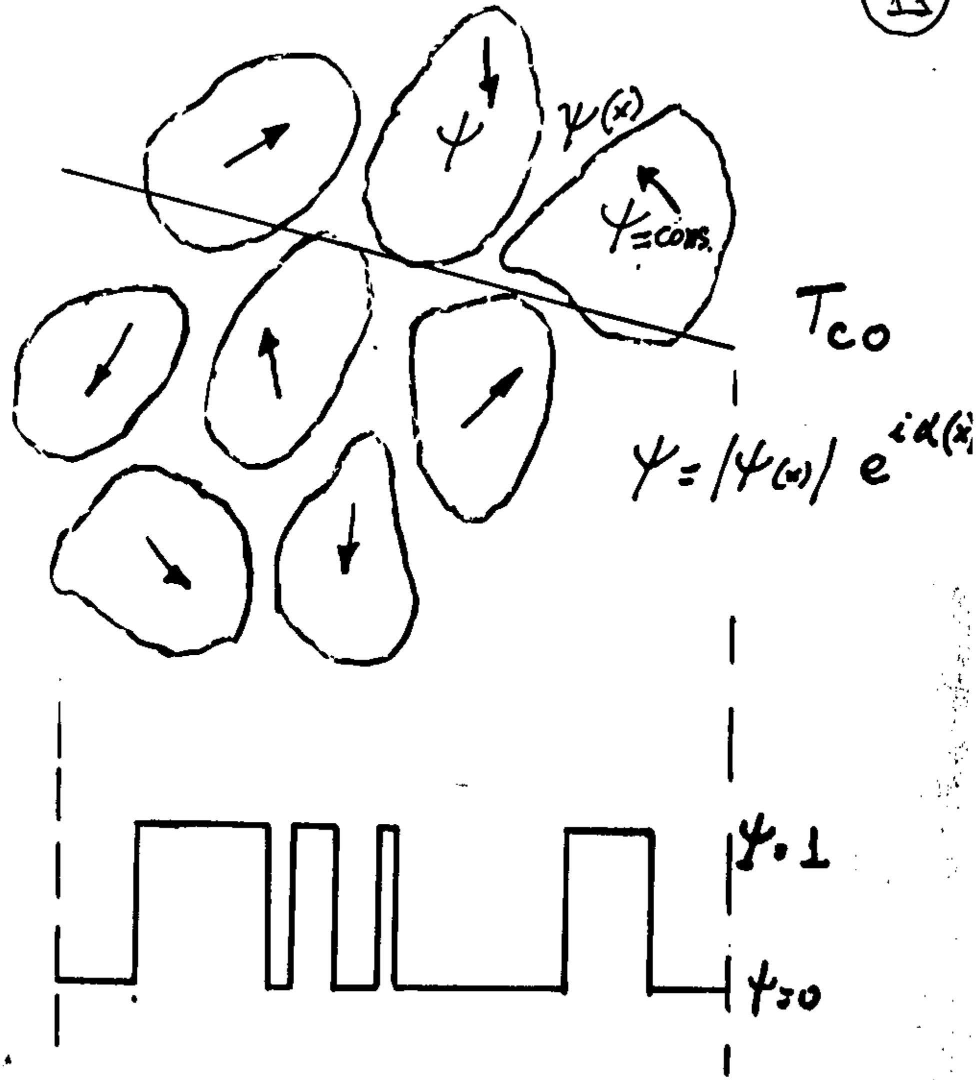

Granular picture at the onset temperature, T_{co}

Modulation of $\Psi(x)$ in distances larger than $\lambda(T)$, at least in one direction.

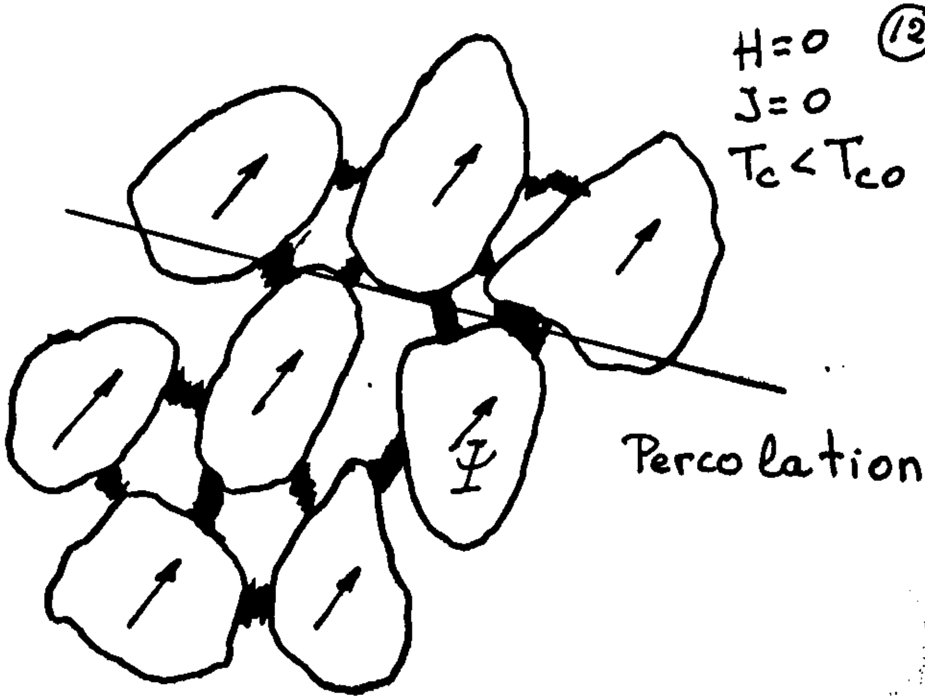

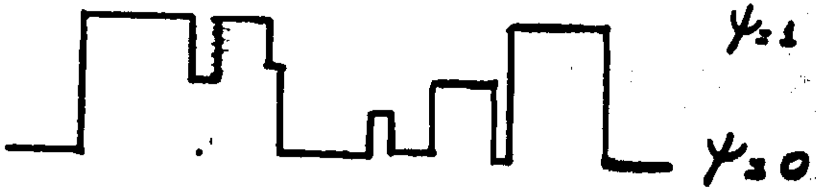

Multiple connected distribution of defects of length > λ

Phase lock at $T_c < T_{co}$

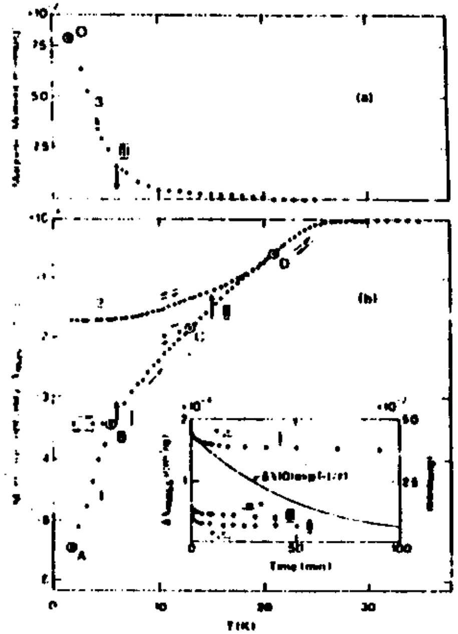

FIG. 2. Flux-trapping curve (3) and nonergodic values vs ergodic behavior of the susceptibility after zero-field and field cooling, respectively, as discussed in the text. Inset: Decay of metastable states, $\tau = 39$ min.

1144

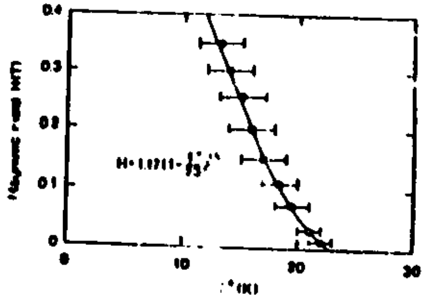

FIG. 3. Experimentally determined $H(T^*)$ line that separates ergodic from nonergodic areas together with an analytic expression for the quasi de Almeida–Thouless line

First Results

15

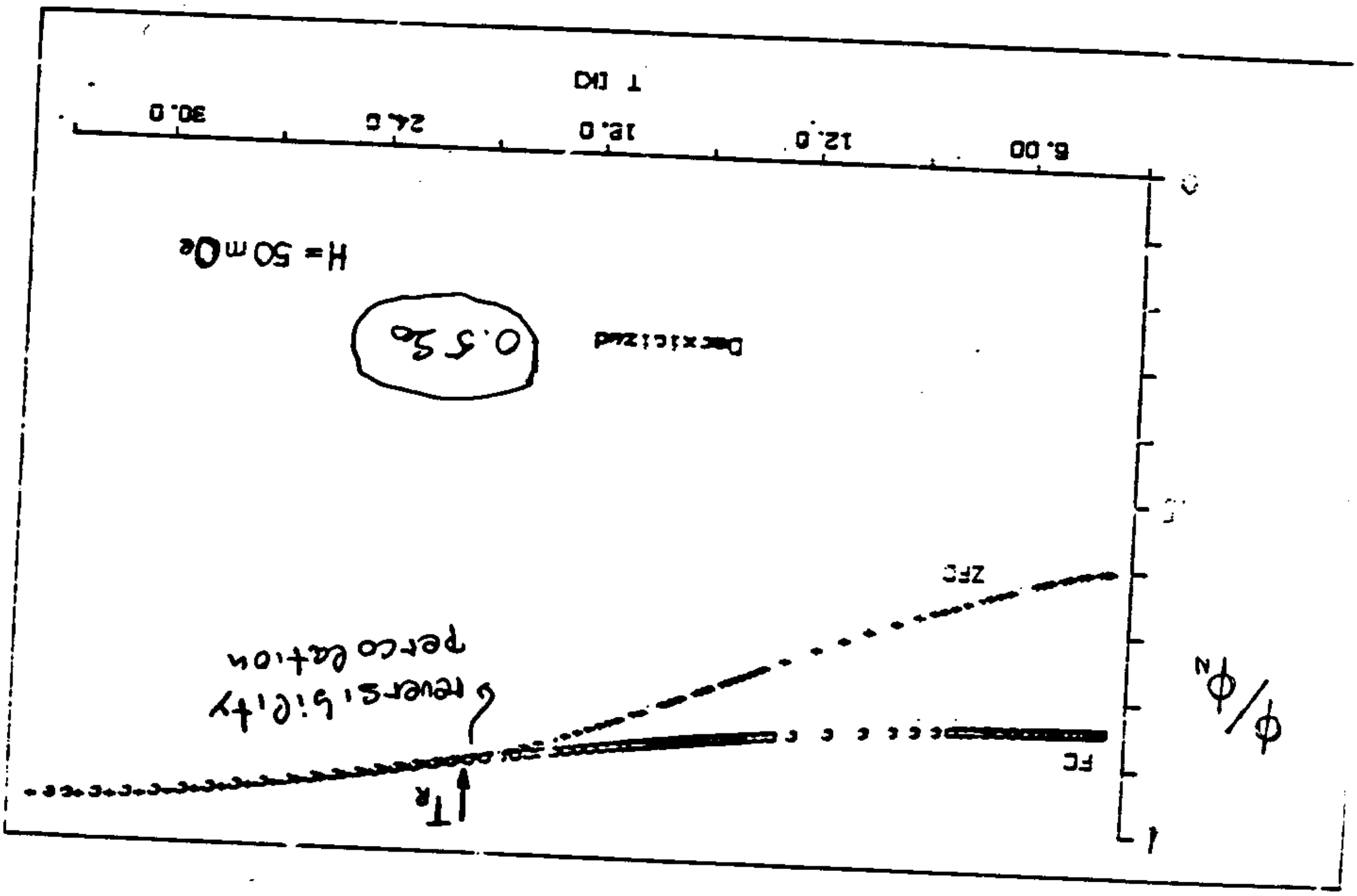

H= 50 mOe
0.5 So
Deoxidized
reversibility percolation
T_R
ZFC
FC
φ/φN
T [K]
6.00
12.0
18.0
24.0
30.0
1
0

14

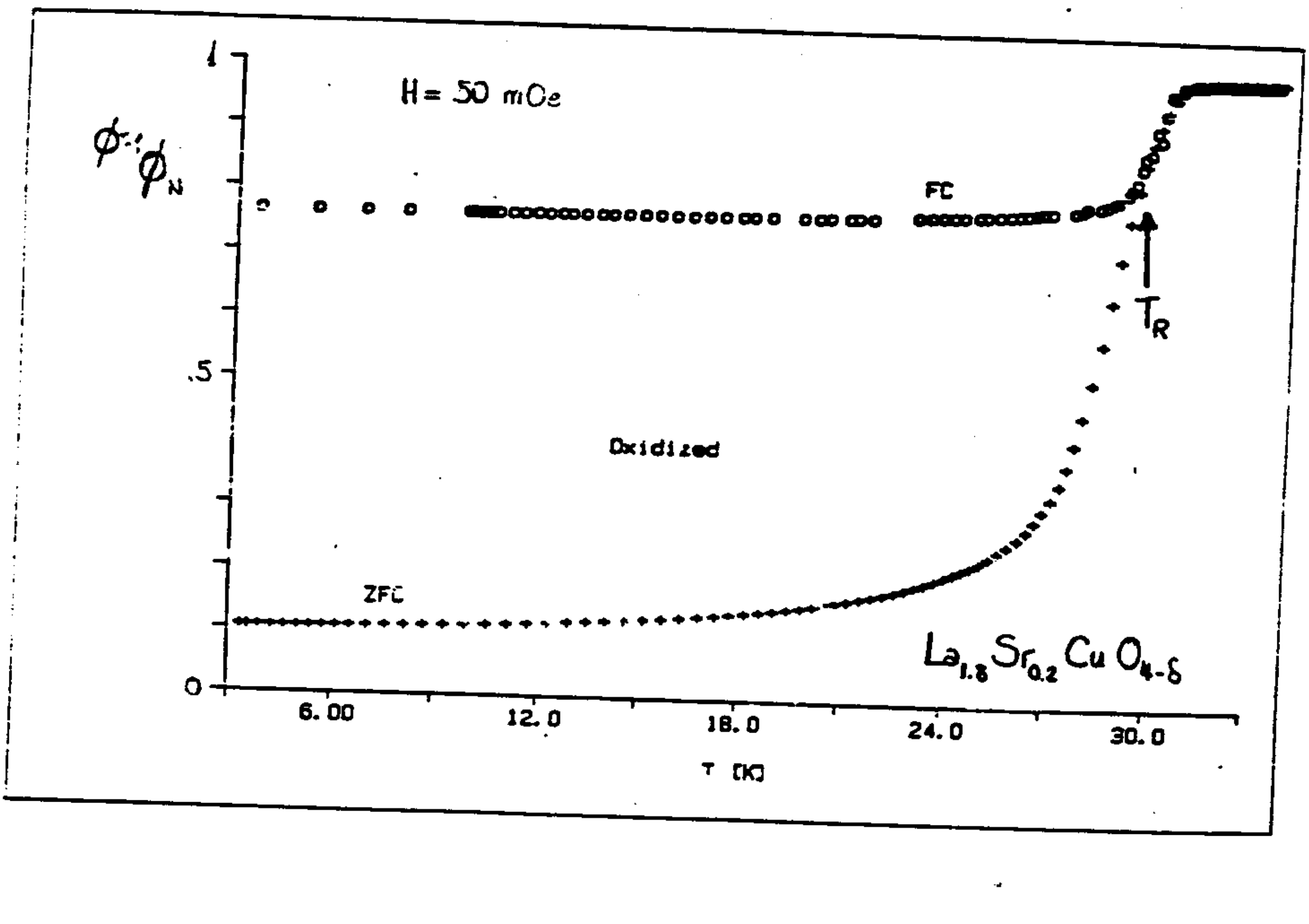

H= 50 mOe
φ/φN
FC
T_R
Oxidized
ZFC
$La_{1.8}Sr_{0.2}CuO_{4-\delta}$
1
.5
0
6.00
12.0
18.0
24.0
30.0
T [K]

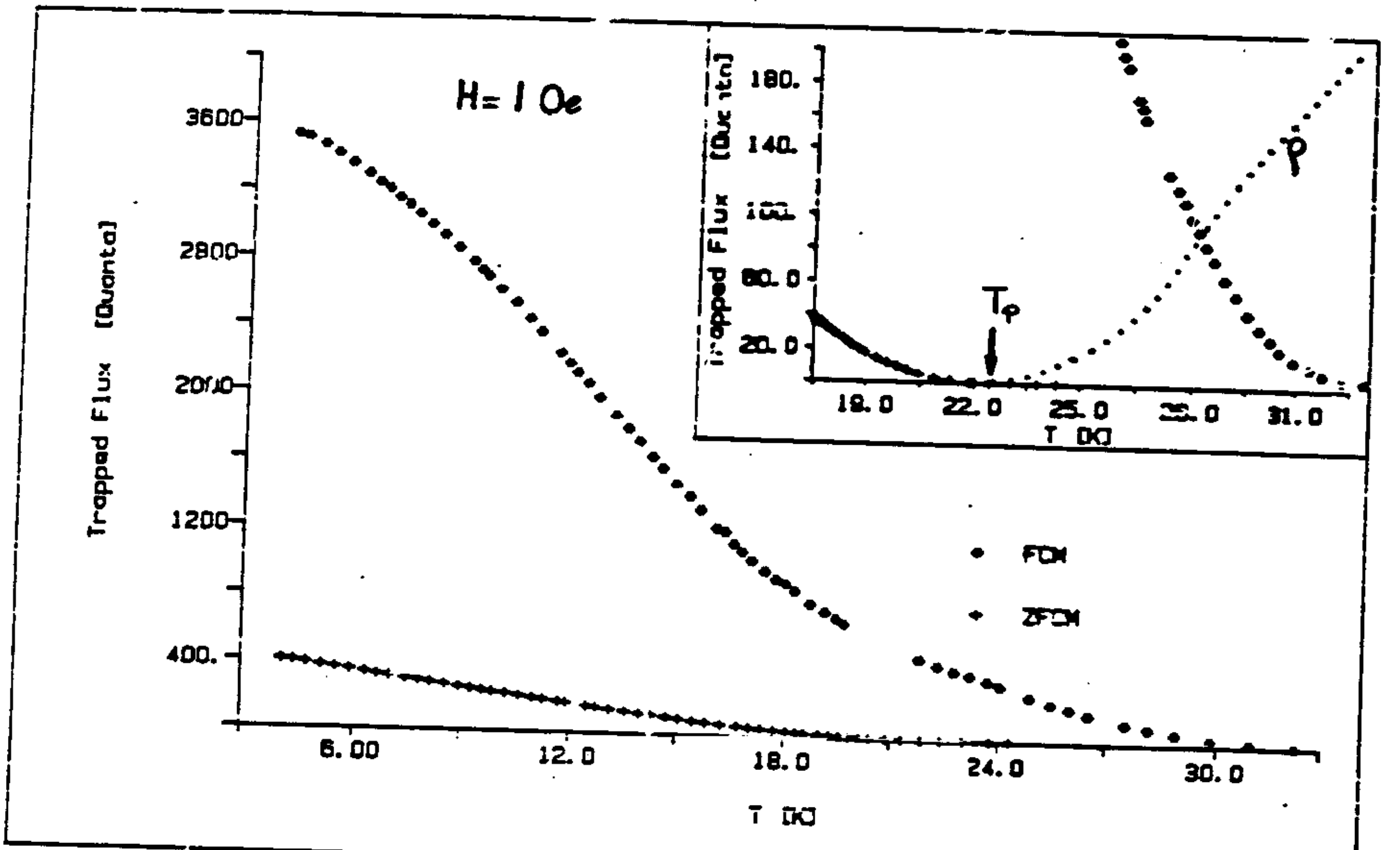

Demonstration of the existance of two materials in 0.5% deoxygenated sample. Measurements of remanent moments at H=0. Notice in inset the resistive percolation

Expanded flux scale T (K) of ZFC of fig 14 showing no full Meissner behavior

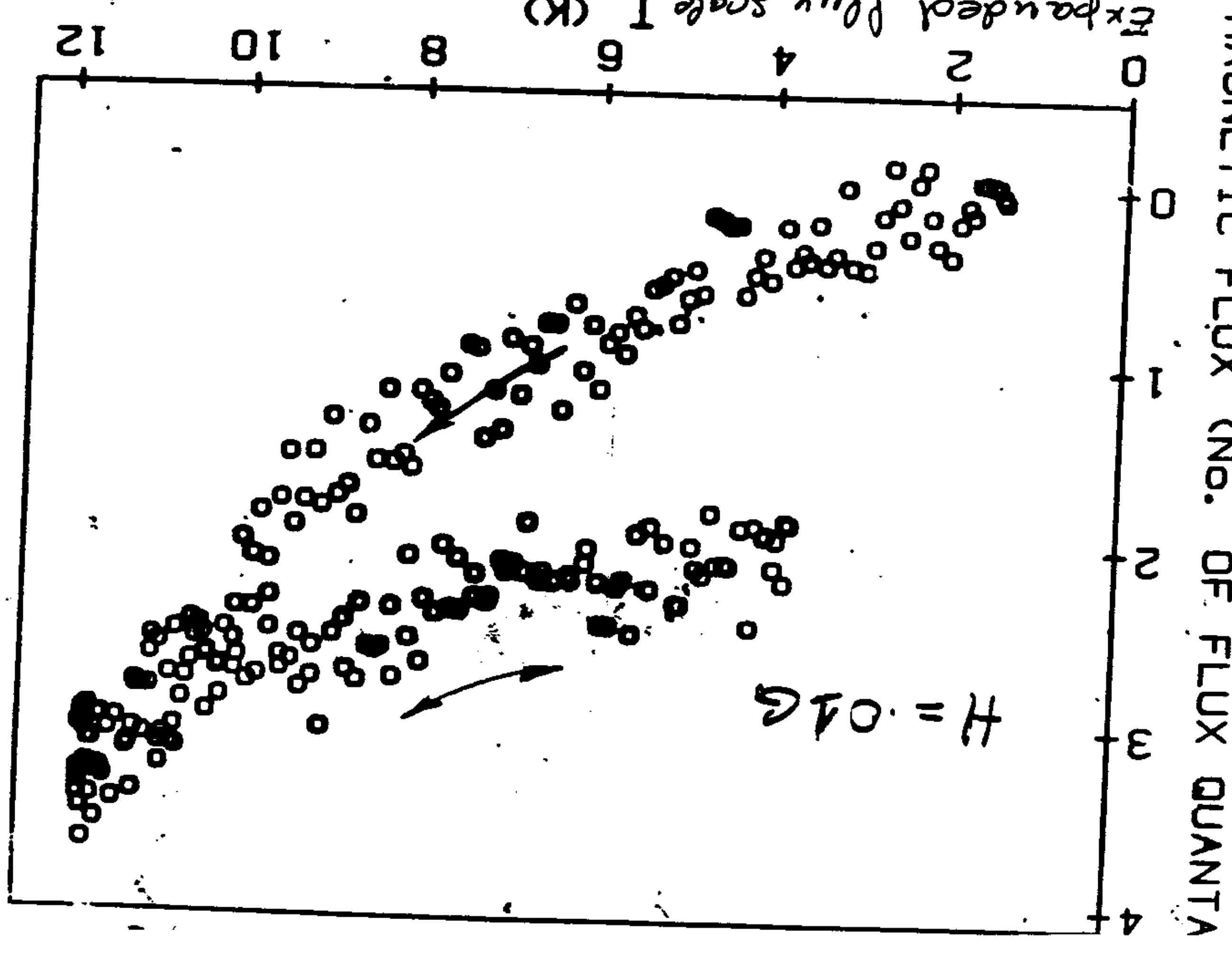

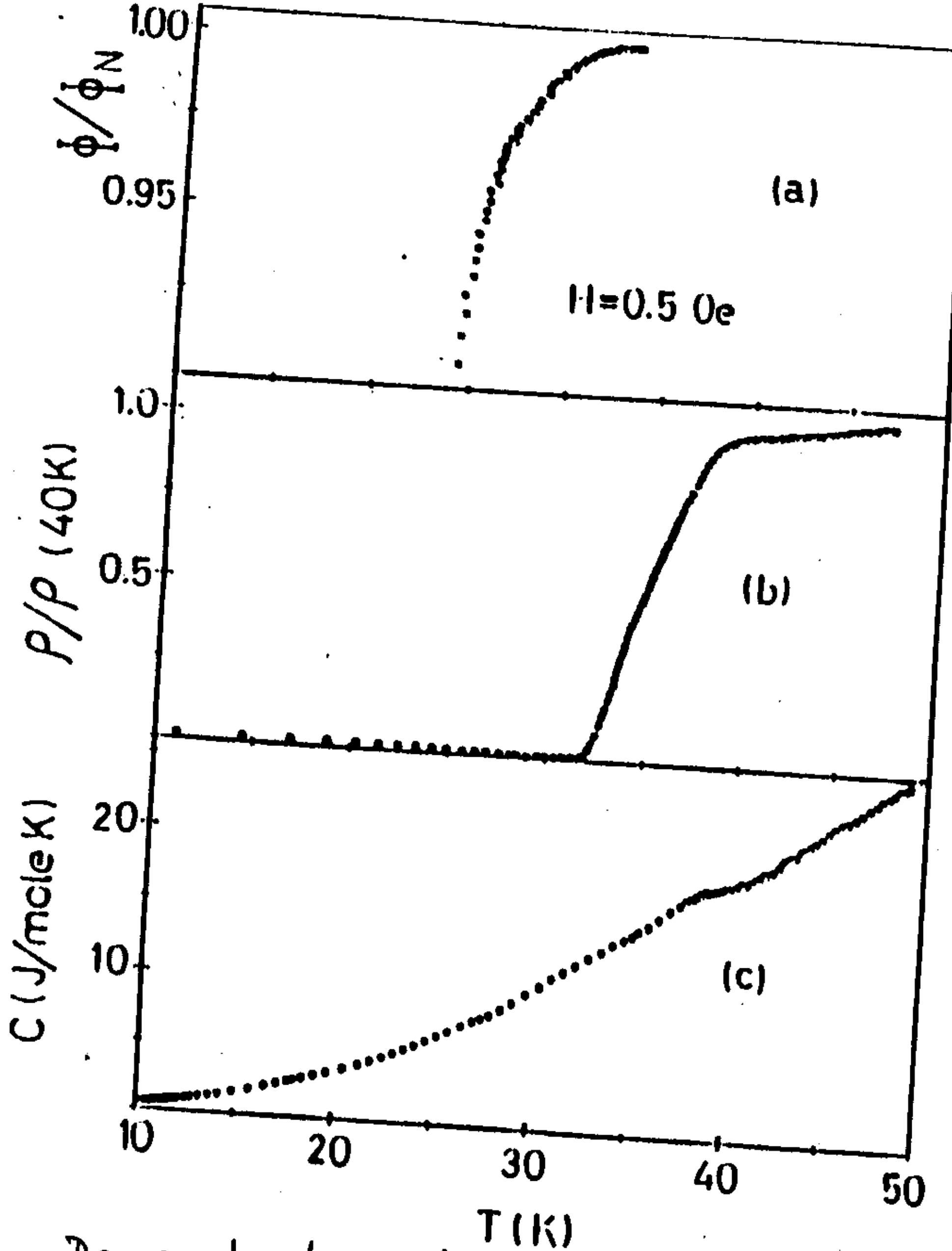

Demonstration of granular behavior La Sr Cu O oxydized sample

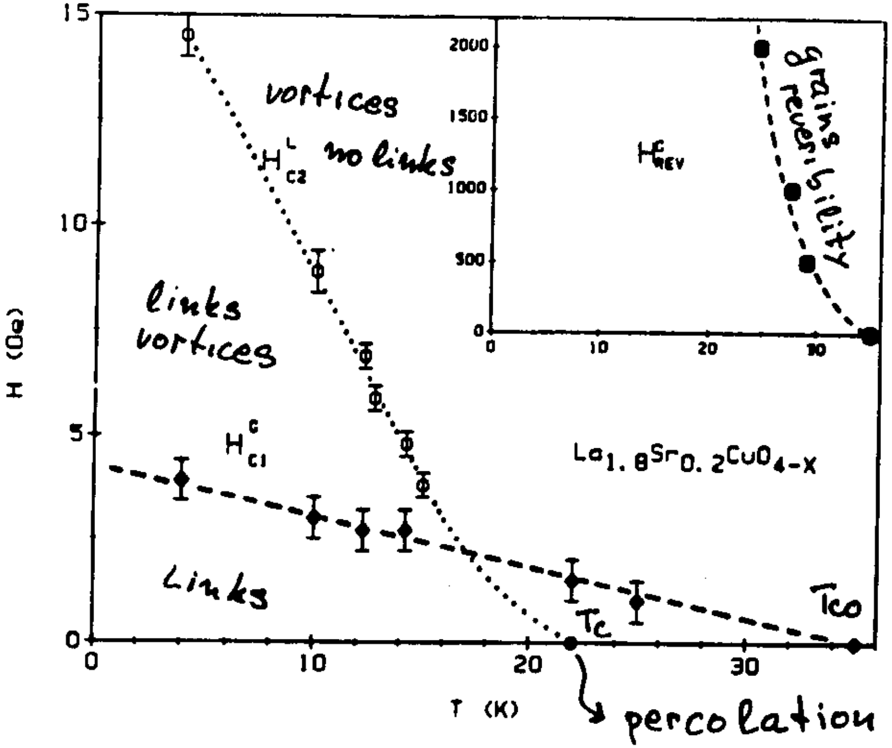

Phase diagram of a deoxydized (0.5%) sample.

Notice depresion of H_{c1} due to modulation of Ψ^2.

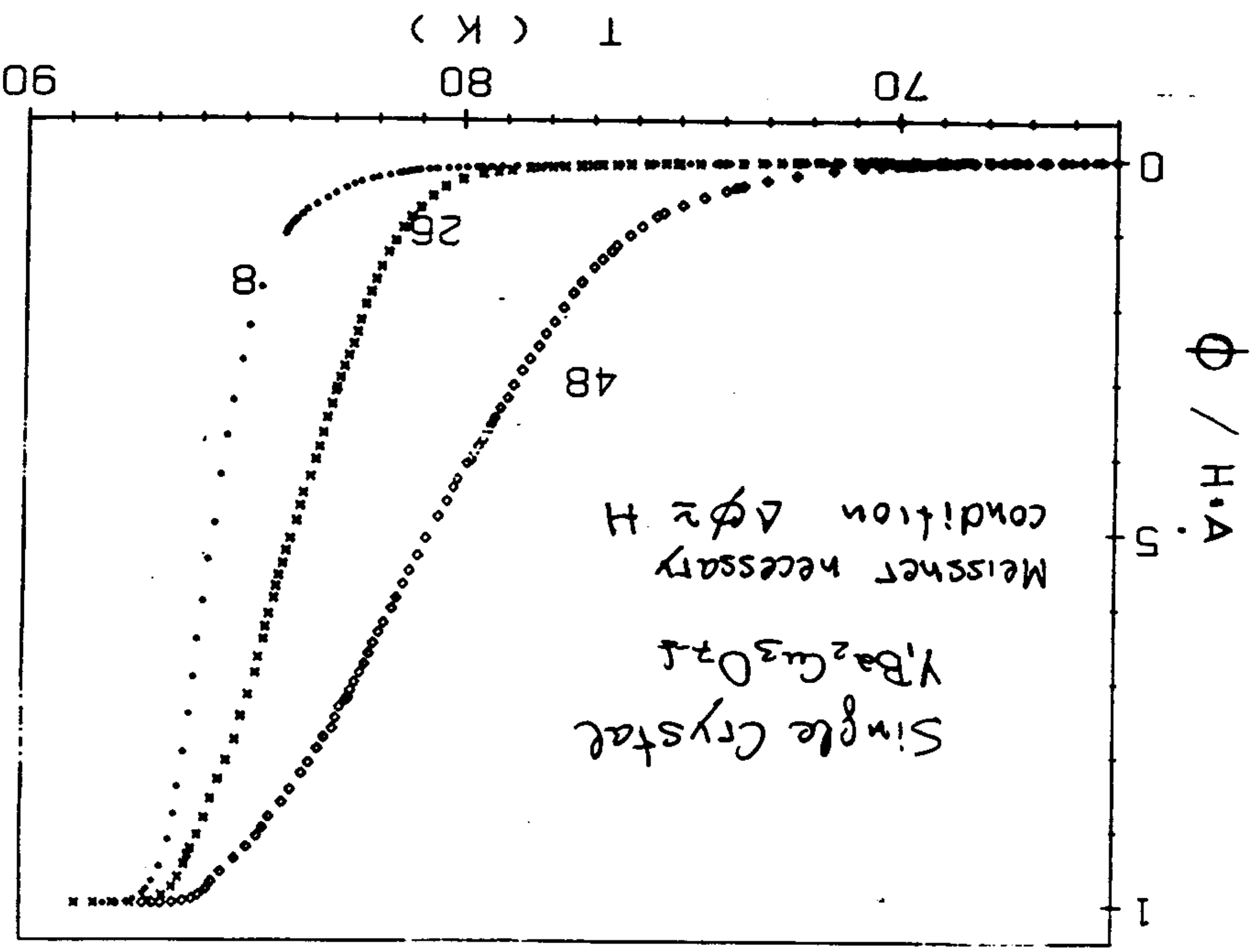

T (K)
90
80
70
0
.5
1
Φ / H·A
8
26
48
Single Crystal
$Y_1Ba_2Cu_3O_{7-\delta}$
Meissner necessary
condition ΔΦ ≈ H

(21)

20

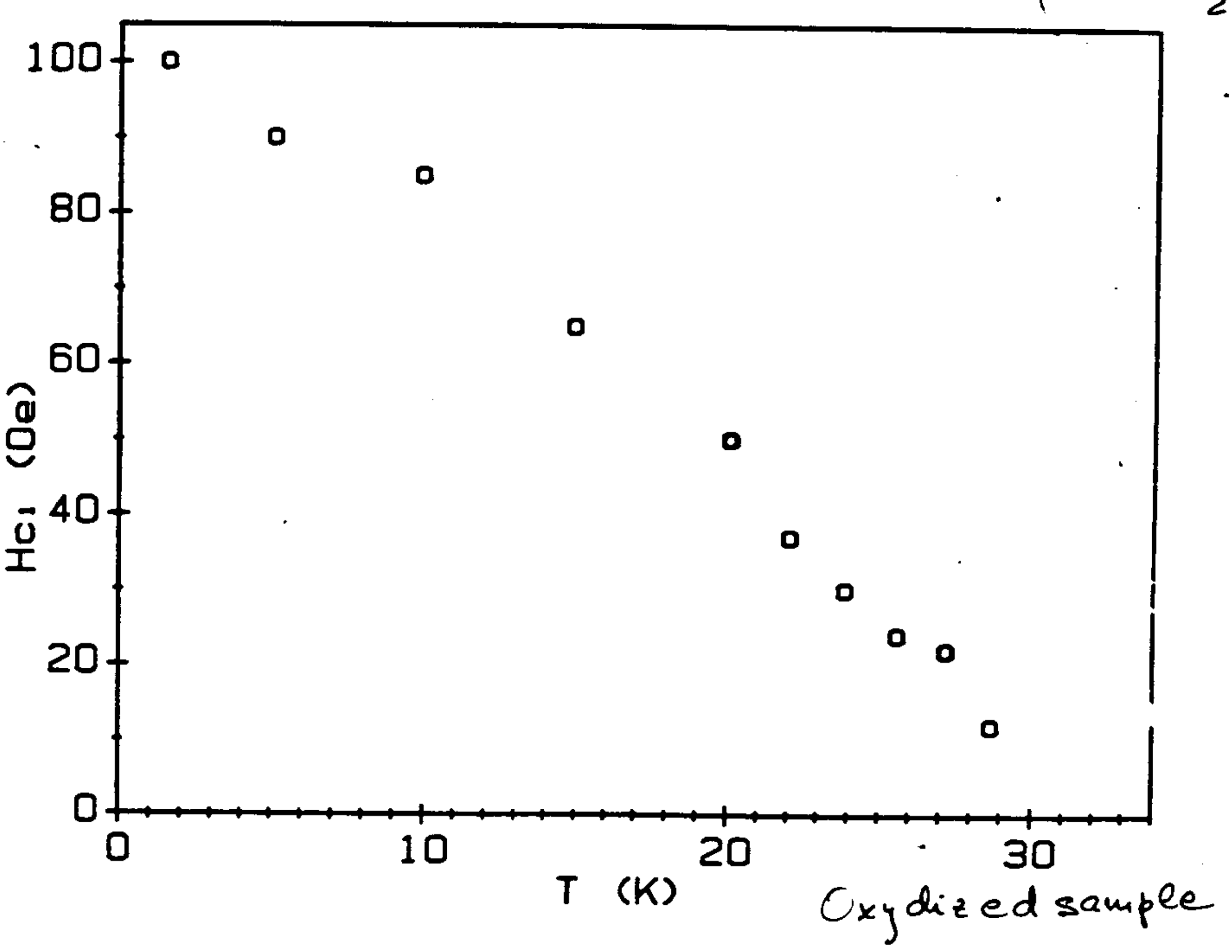

Hc1 (Oe)
100
80
60
40
20
0
0
10
20
30
T (K)
Oxydized sample

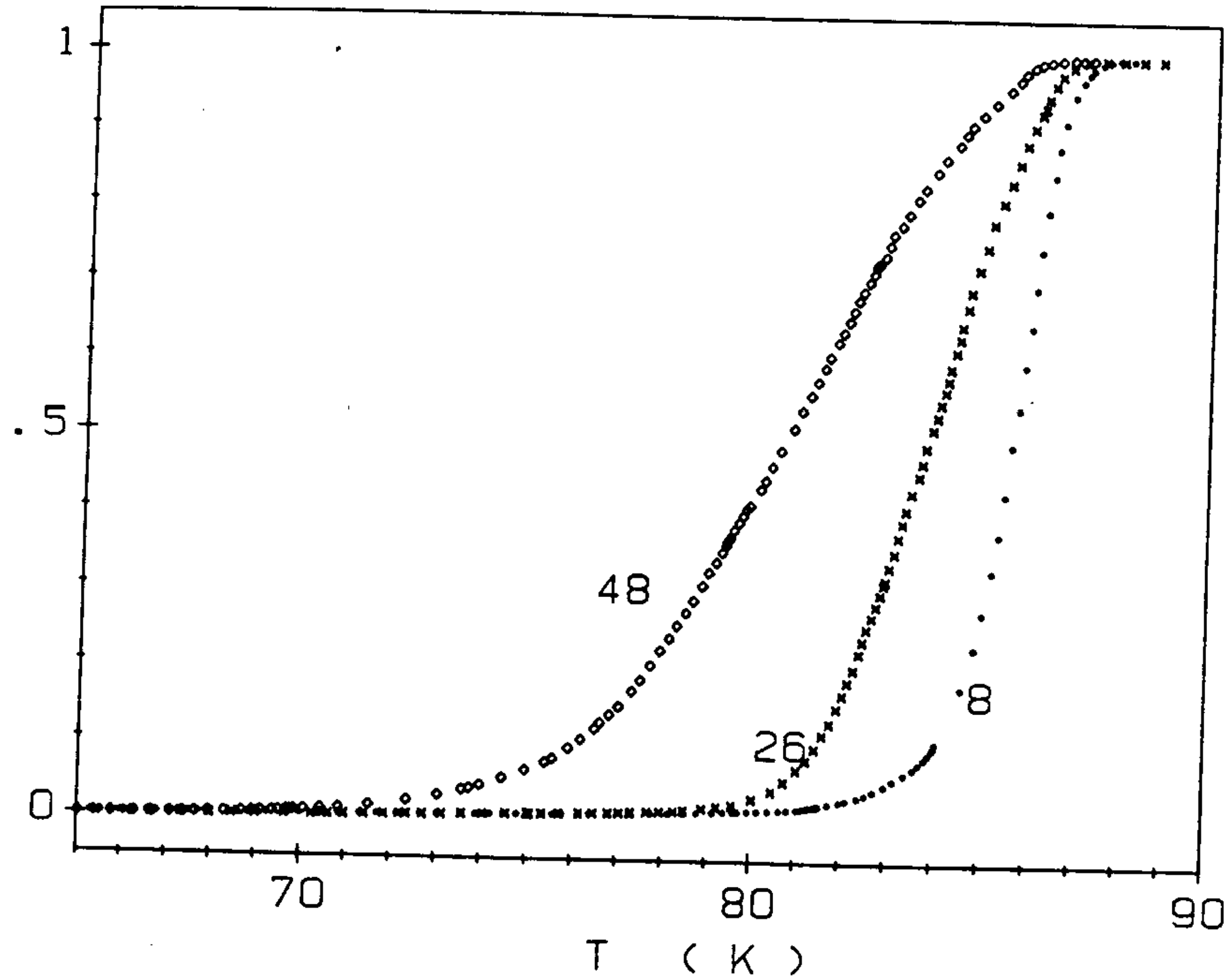

1
.5
0
48
26
8
70
80
90
T (K)

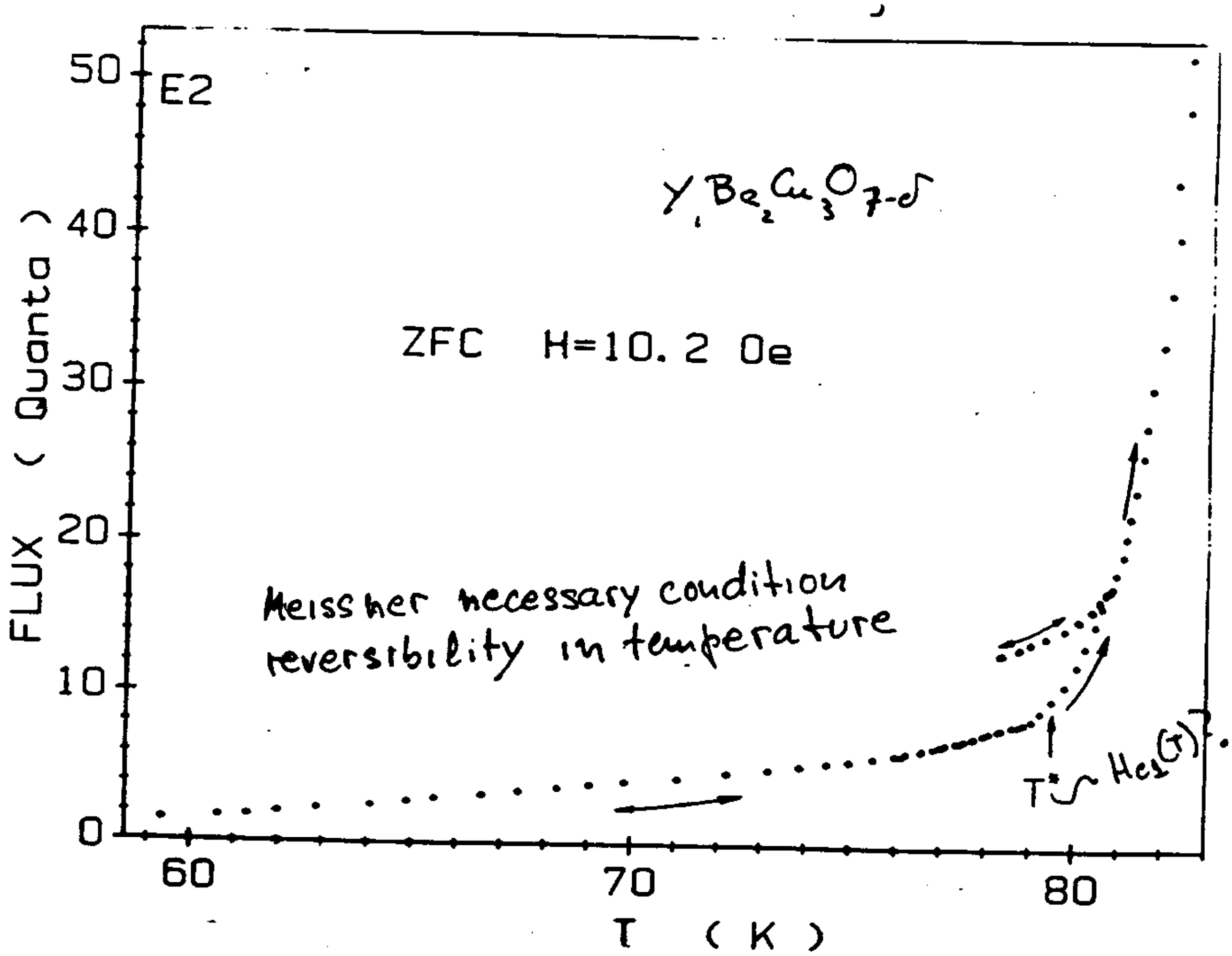

E2
Y1Ba2Cu3O7-δ
ZFC H=10.2 Oe
Meissner necessary condition
reversibility in temperature
T* ~ Hc1(T)?
FLUX (Quanta)
50
40
30
20
10
0
60
70
80
T (K)

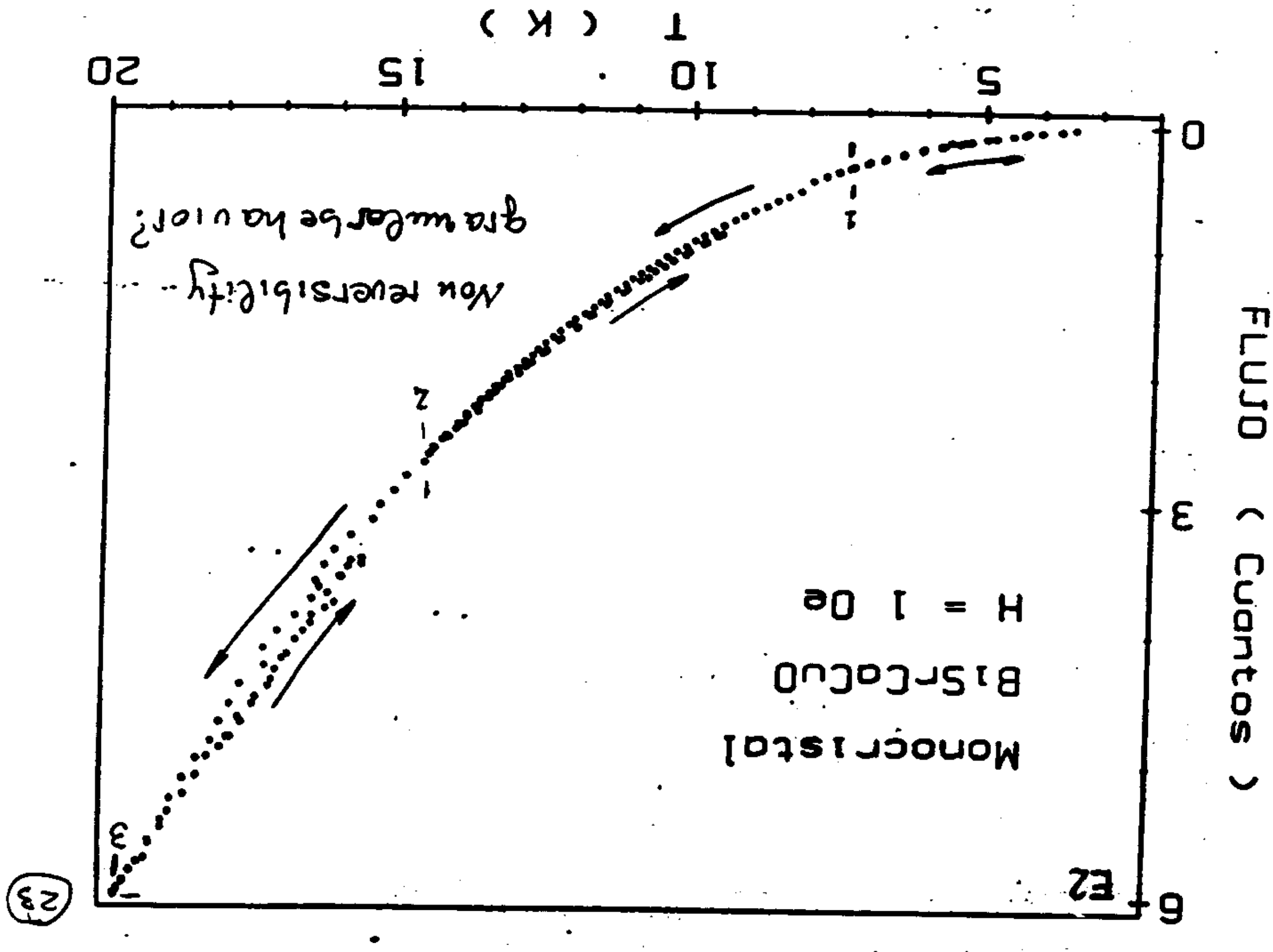
T (K)
20
15
10
5
0
3
6
FLUJO (Cuantos)
Monocristal
BiSrCaCuO
H = 1 Oe
E2
Non reversibility
granular behavior?
23

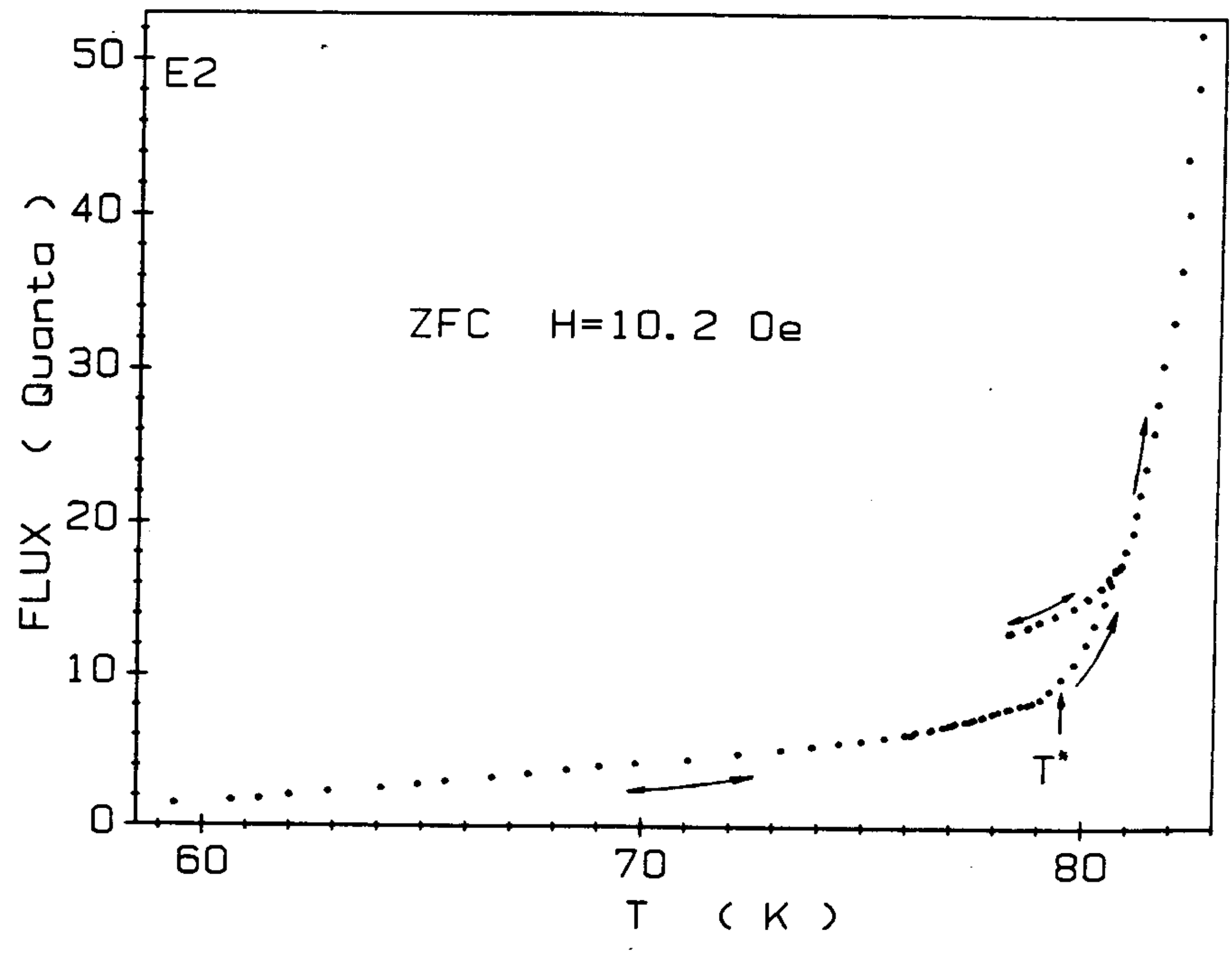
FLUX (Quanta)
0
10
20
30
40
50
E2
ZFC H=10.2 Oe
T*
60
70
80
T (K)

(24)

FIG 2

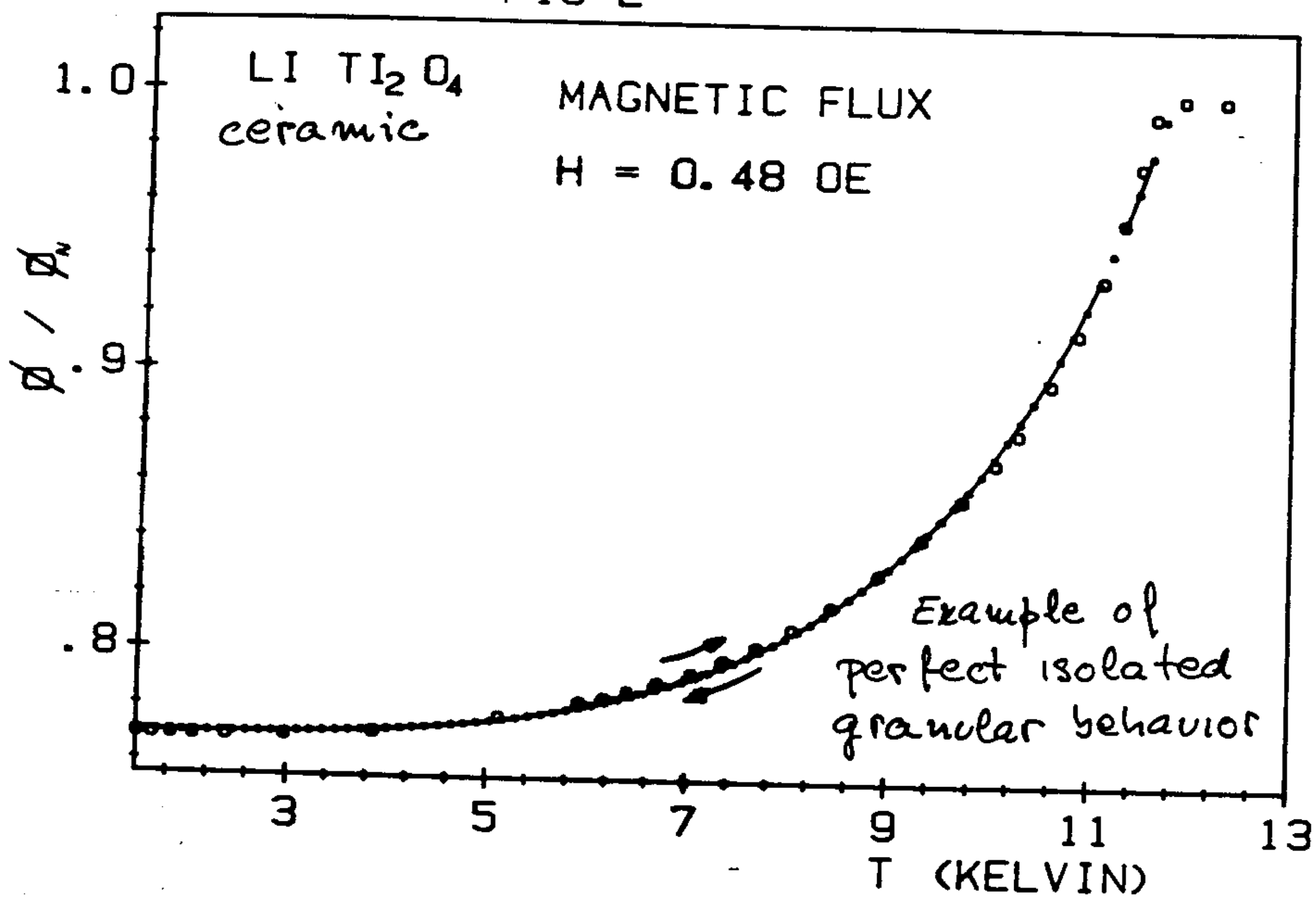

LI TI_2O_4
ceramic
MAGNETIC FLUX
H = 0.48 OE
Example of perfect isolated granular behavior
Ø / Øₙ
1.0
.9
.8
3
5
7
9
11
13
T (KELVIN)

(25)

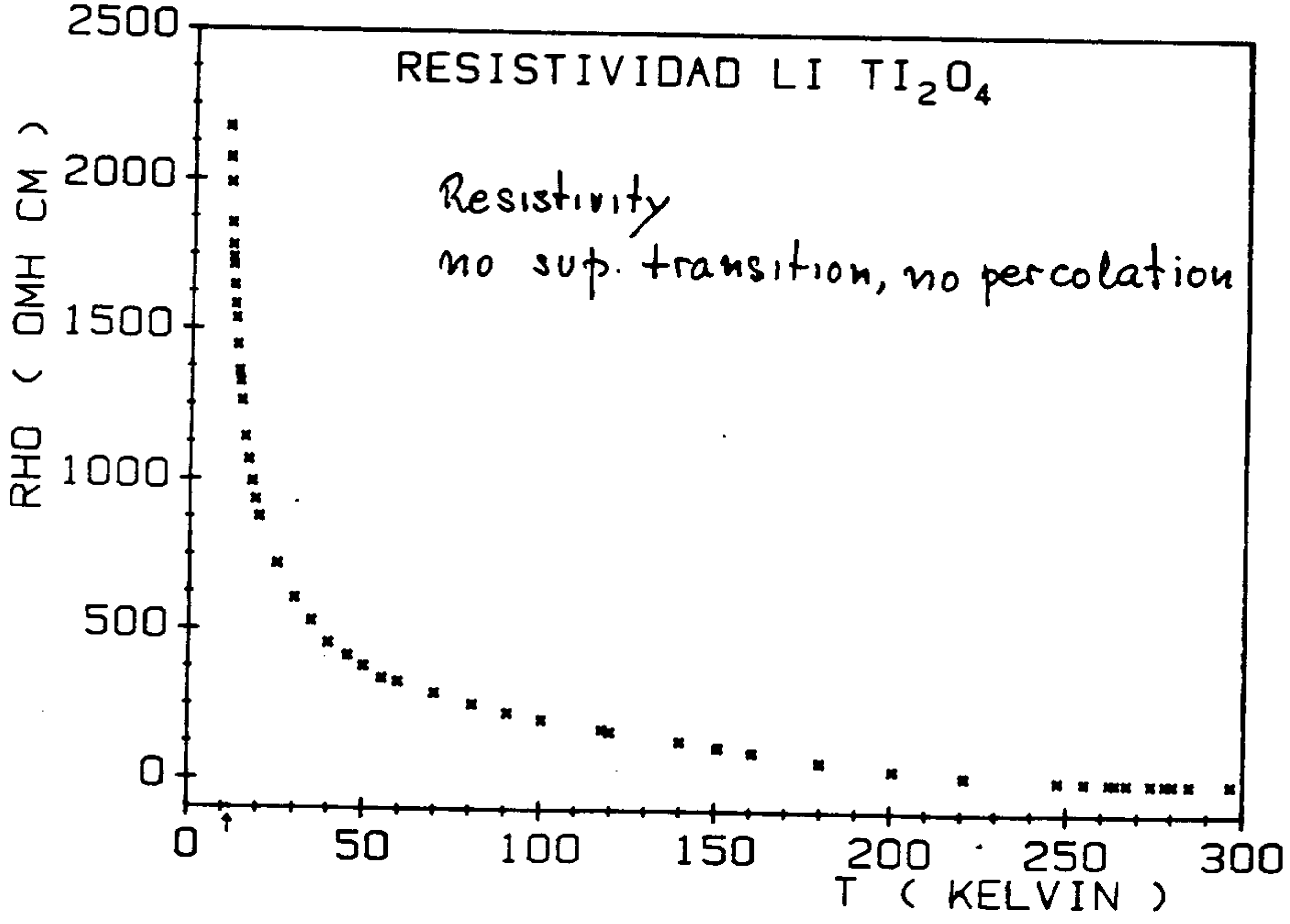

RESISTIVIDAD LI TI_2O_4
Resistivity
no sup. transition, no percolation
RHO (OMH CM)
2500
2000
1500
1000
500
0
0
50
100
150
200
250
300
T (KELVIN)

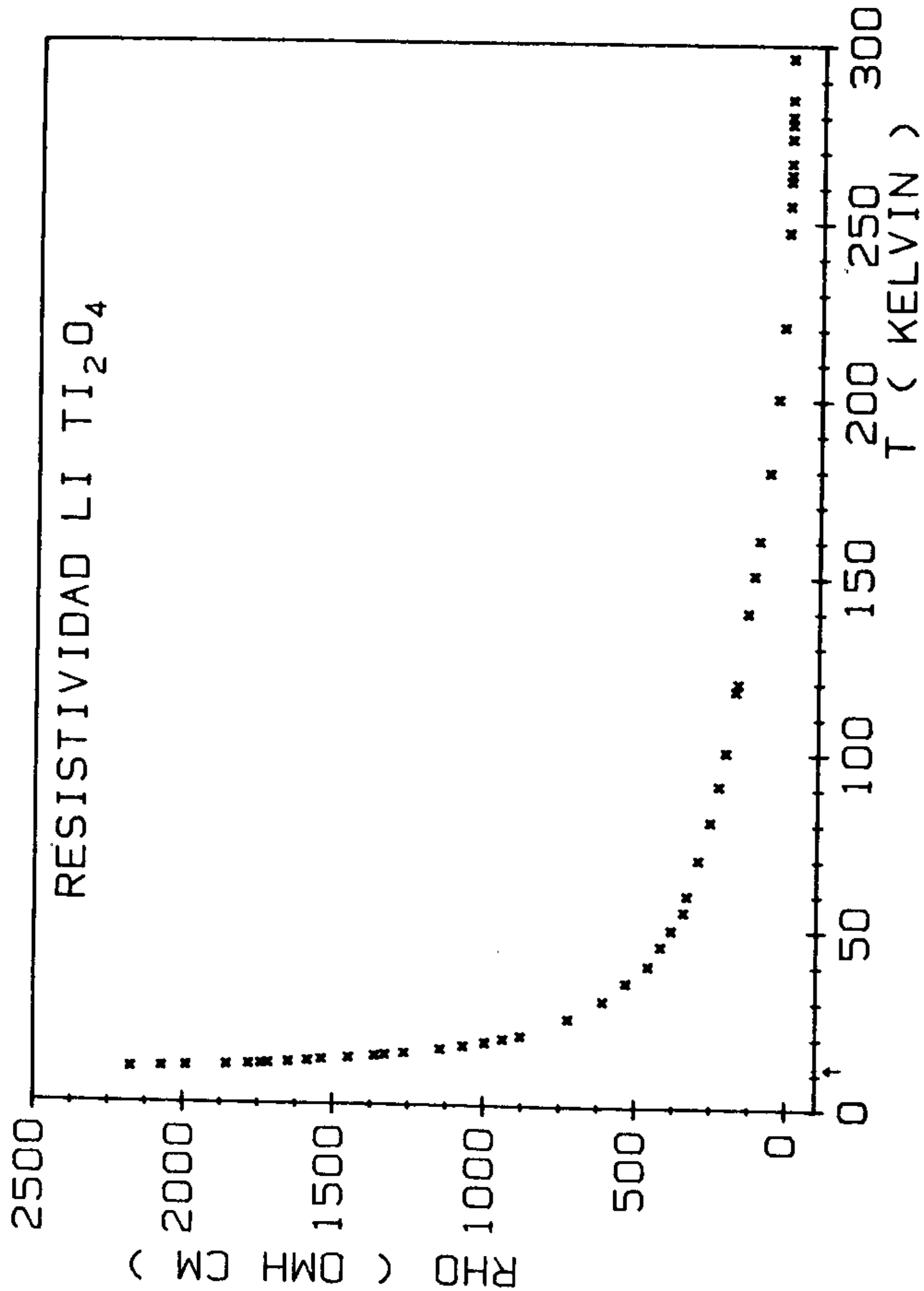

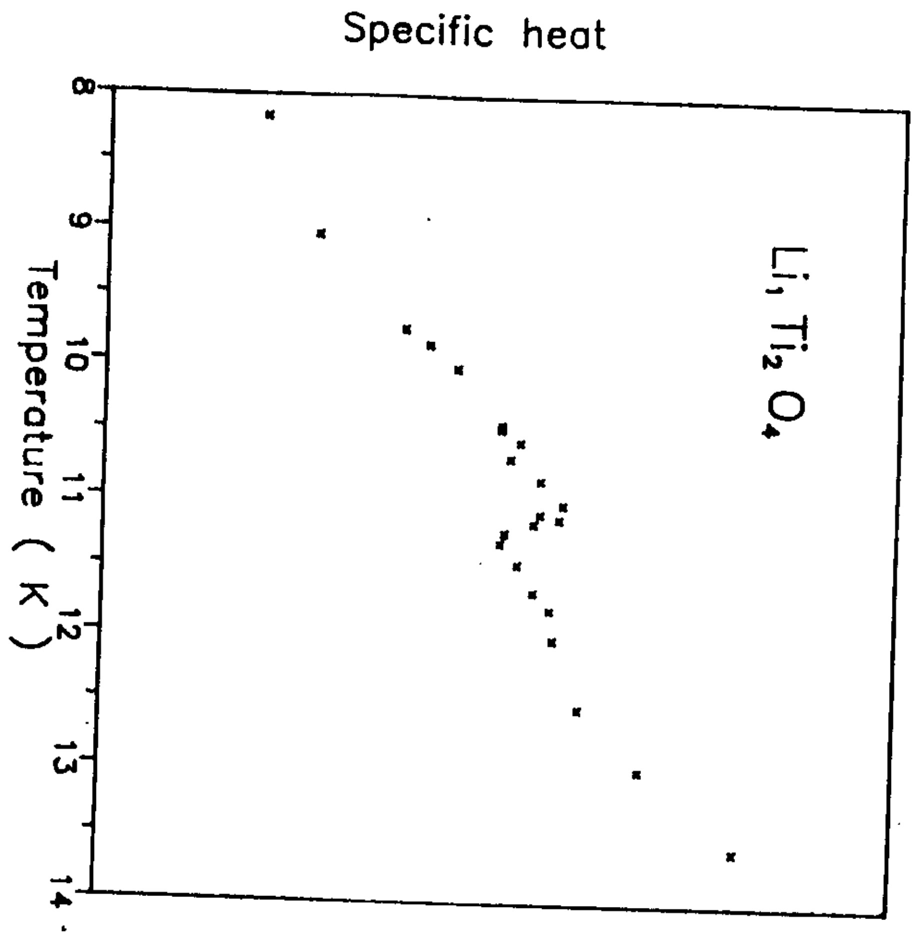

isolated grain behavior

Superconducting transition
no electrical percolation

(27)

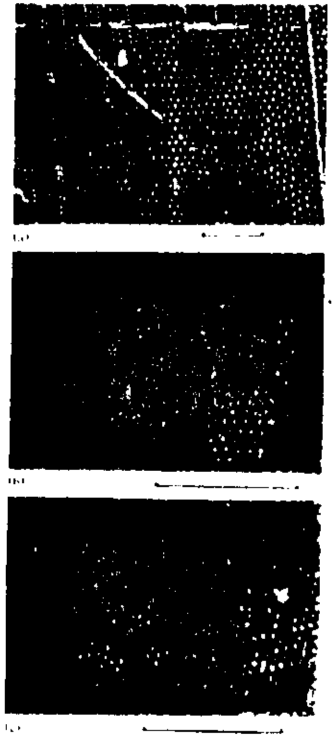

FIG. 1. The vortex pattern in twin-free regions of $YBa_2Cu_3O_7$ crystals cooled in fields of 20, 40, and 80 G to produce local fields of about 15, 35, and 65 G in the areas shown. The markers are 10 μm.

order increases with B, a test that failed in Gammel *et al.* Here order increases with field as indicated, somewhat inadequately, in Figs. 1(b) and 1(c). The ordered lattice extends far beyond the areas shown and is greater for the higher field as in conventional superconductors.

Figure 2 shows a more densely twinned area of the sample cooled at 20 G. Vertical strings of vortices delineate the twin boundaries. The coincidence of the vortex strings with twin boundaries all over the sample was verified by polarized light microscopy. The overall correspondence leads us to conclude that the "twin-free" regions are just that, and not just regions where twins are unresolved optically. Also, there is evidence that the vortices are pinned in, not against, the boundaries, i.e., the boundaries are potential minima. For example, vortex densities greater than the applied field occur at some boundaries, and vortices are found at locations where local vortex densities imply they would not be held unless

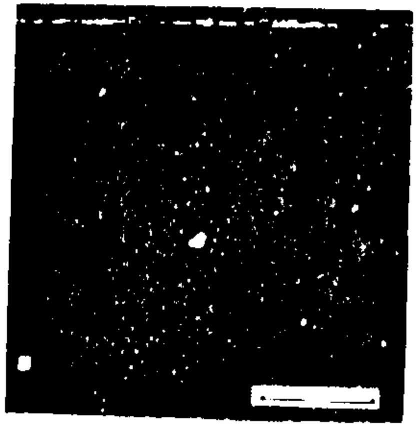

FIG. 2. The vortex pattern in a more highly twinned region for the sample cooled at 20 G. The marker is 10 μm.

they were at a minimum. Such a case will be shown below. The vortex strings are an accident of the approximate commensuration of the vortex spacing and the twin boundary spacing in this example, $s \approx a_0$. It should be clear that a somewhat smaller twin boundary spacing would produce a disordered array without such clearly expressed lines. We believe this was the case for Gammel *et al.*

Figure 3 and 4 show the vortex pattern near parts of the edge of the sample cooled at 40 G. Here flux gradients are largest. There is a vortex-free belt near the sample edge which is remarkably well defined except where twin boundaries (Fig. 4) have held vortices in the

FIG. 4. The vortex pattern [illegible] the edge (black line) of the sample cooled at 40 G [illegible] after the field was re[illegible]

Vortices in high Tc

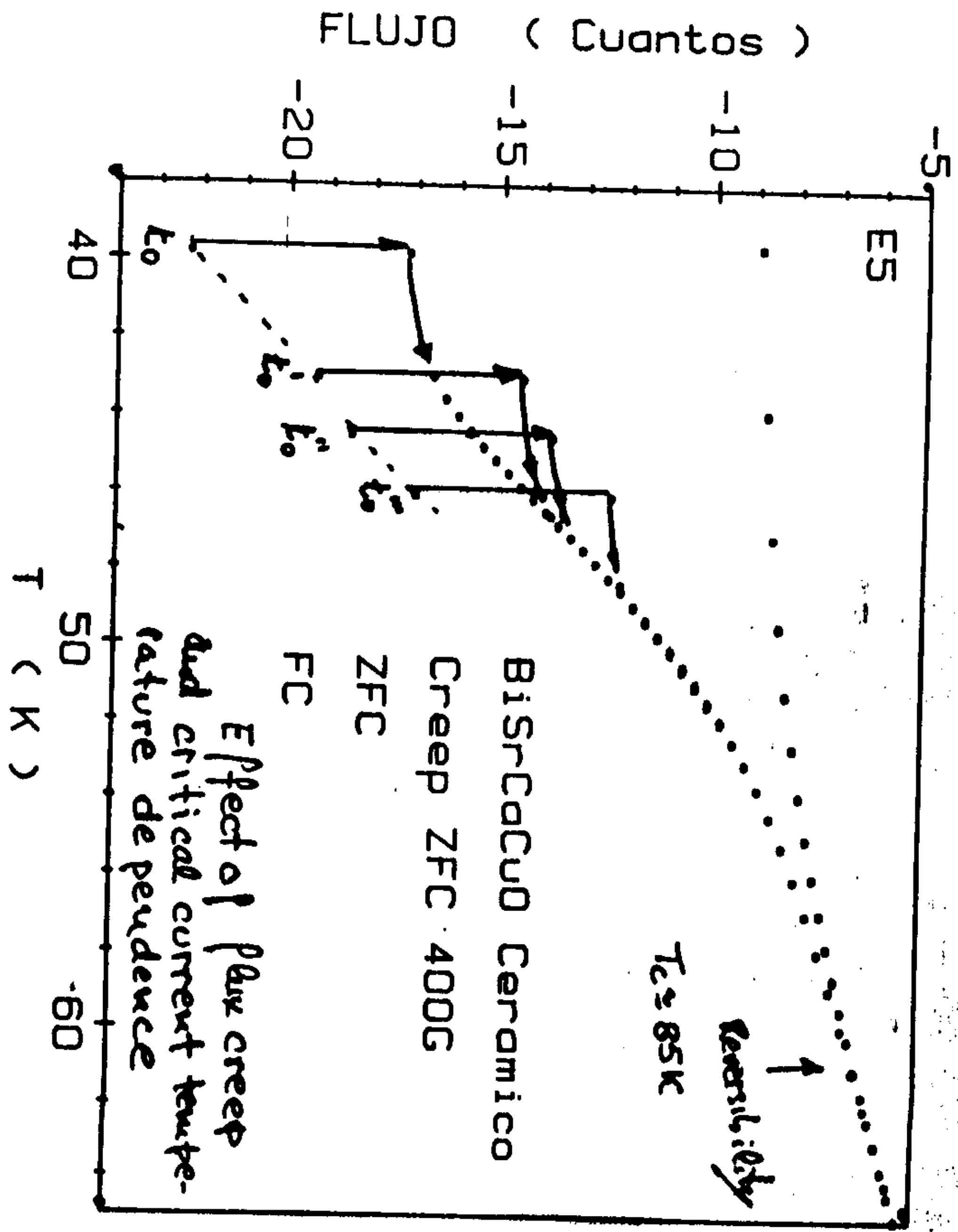

24

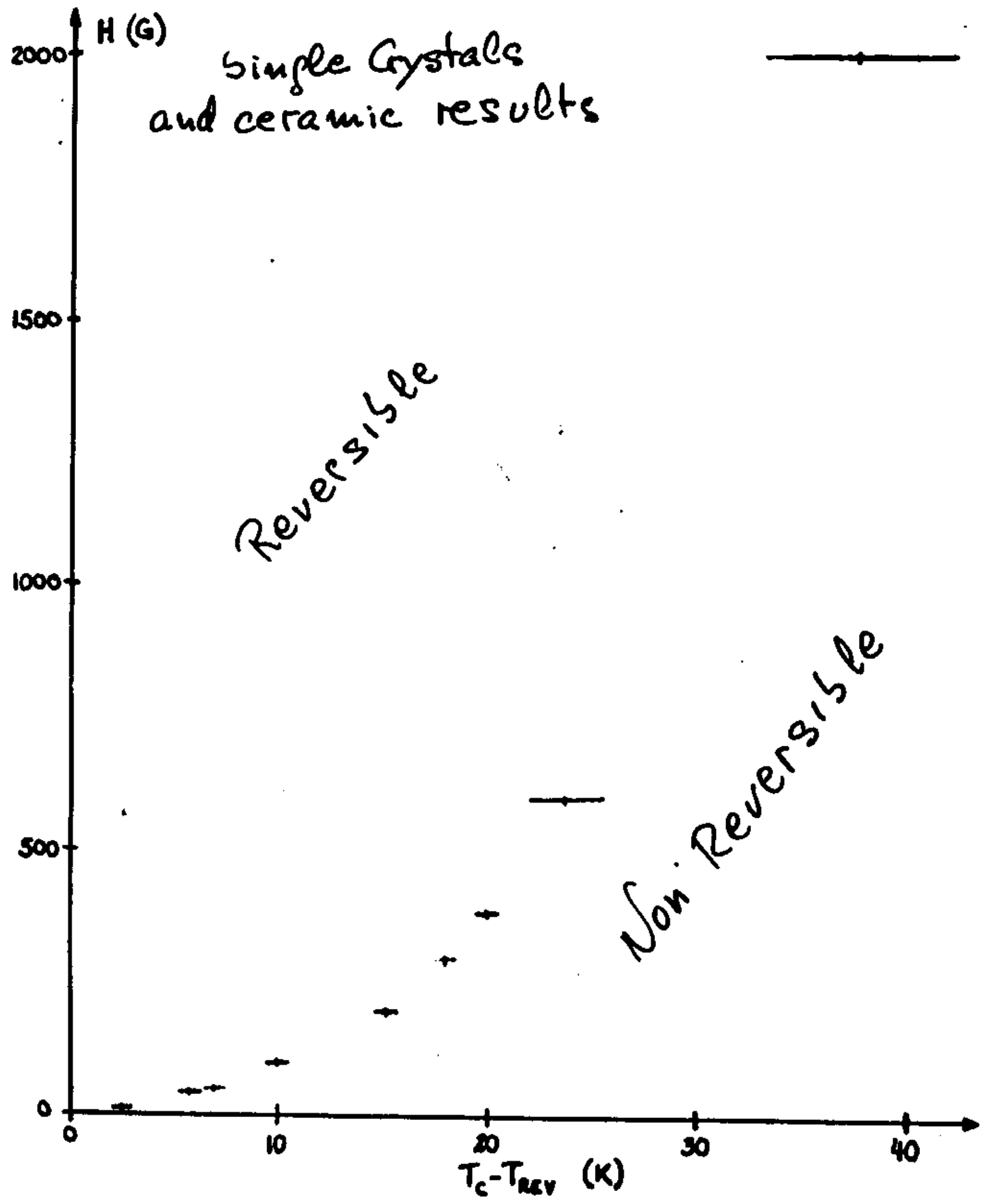

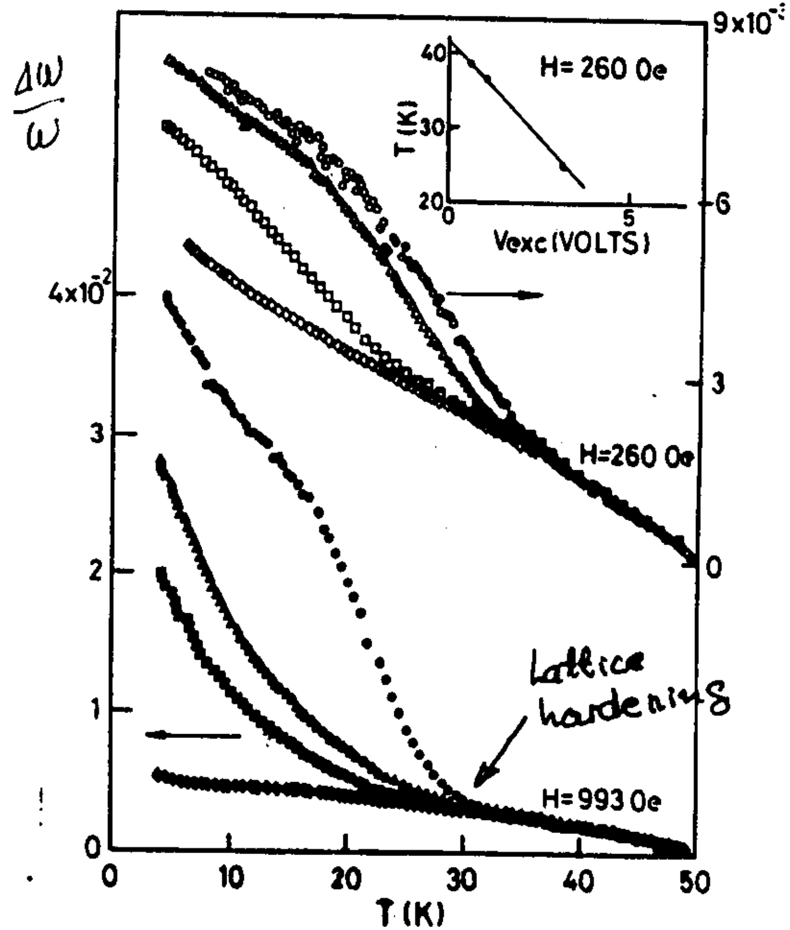

vibrating reed results for Bi Sr Ca Cu O ceramic

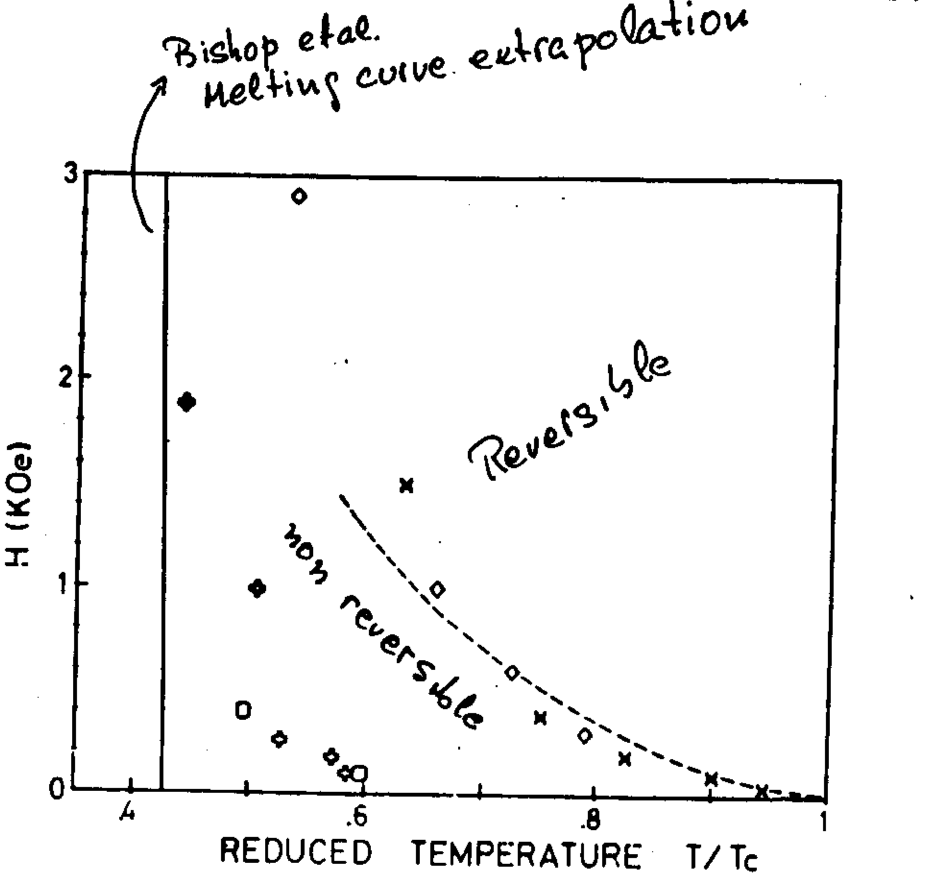

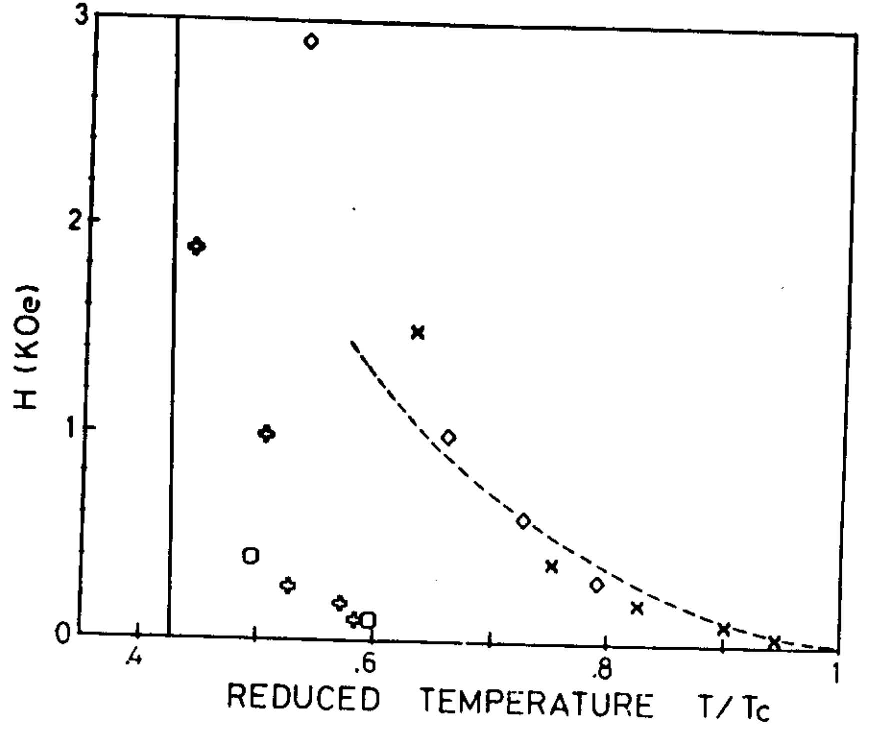

Phase diagram for BiSrCaCuO

+, □ flux lattice hardening

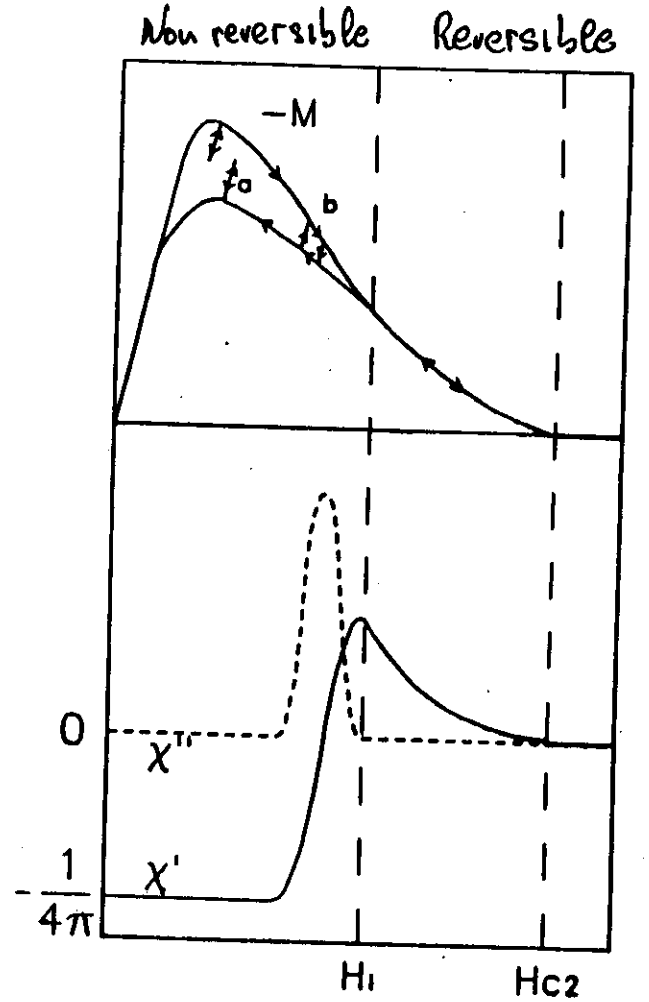

Proposed behavior for dc and ac response

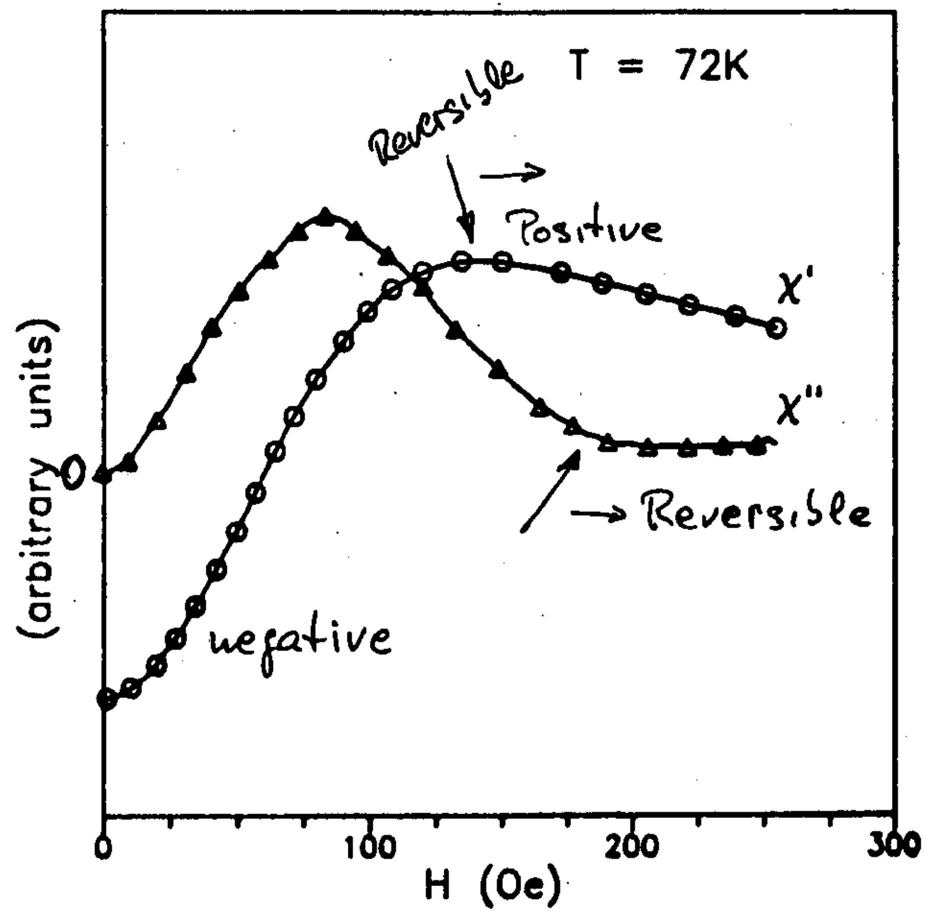

Proof of reversible behavior

30

Fig. 2

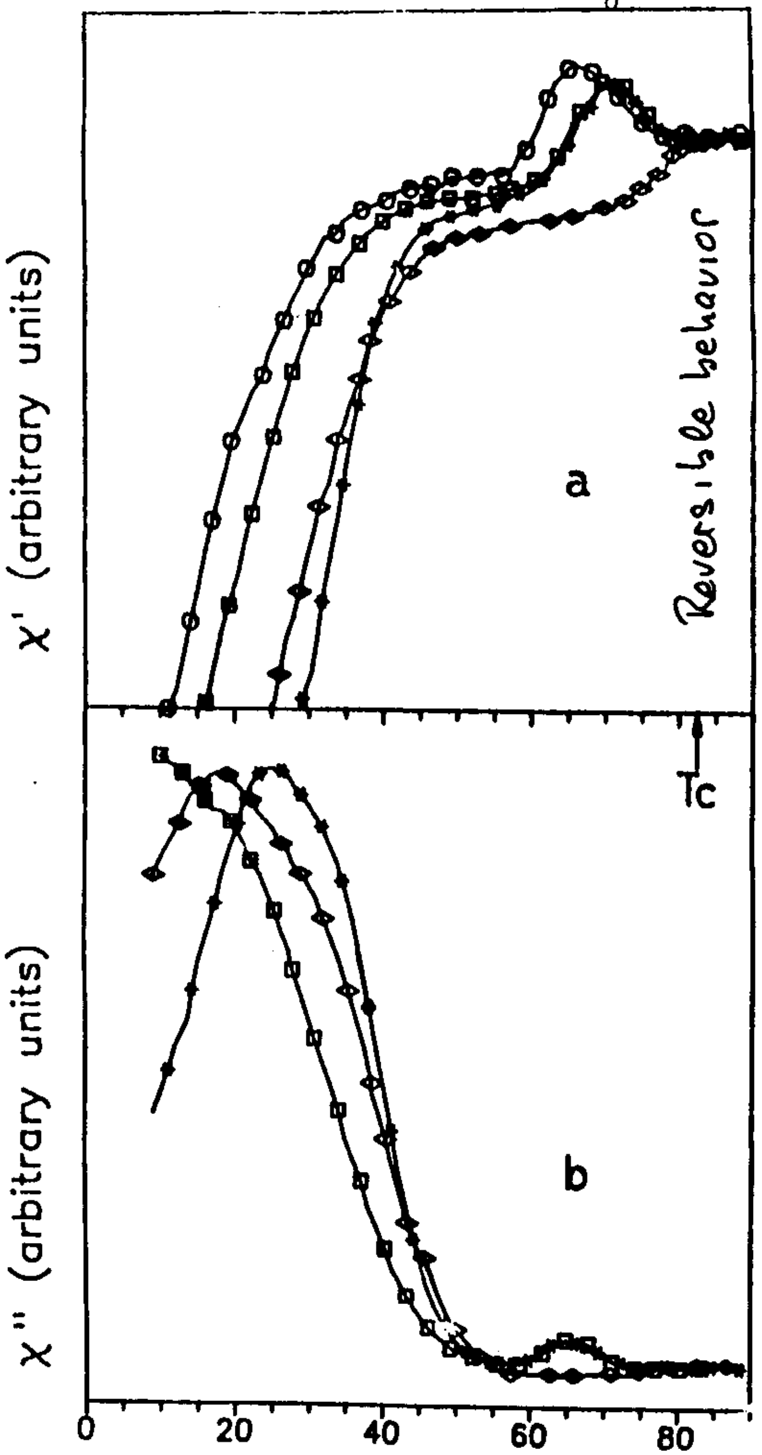

(31)

Fig. 3

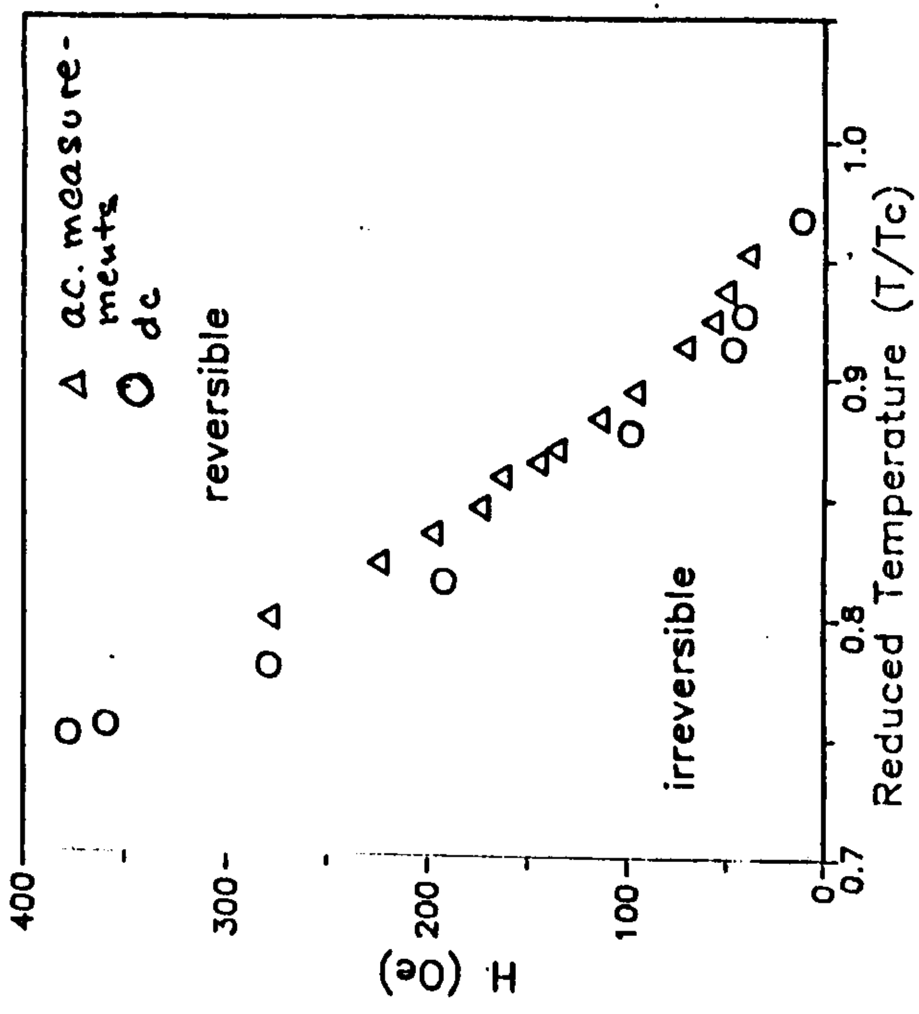

Ceramics what to do?

Flux Creep Interaction

Flux " Time Dependence

Classical Percolation – Reversibility Line

Powders

Individual Flux Pinning

Surface Pinning

Flux Creep in the limit of low number of vortices

S. cristals

Penetration depth and H_{c1}

Solid – Amorphous – Liquid

Defects – Disorder – Transition

Magnetic – Phase – Diagram

Melting – Reversibility